Visual Odometry from Two Point Correspondences and Initial Automatic Camera Tilt Calibration

Mårten Wadenbäck[1], Martin Karlsson[2], Anders Heyden[1], Anders Robertsson[2] and Rolf Johansson[2]

[1] *Centre for Mathematical Sciences, Lund University, Lund, Sweden*

[2] *Department of Automatic Control, Lund University, Lund, Sweden*

Keywords: Visual Odometry, Tilted Camera, Trajectory Recovery.

Abstract: Ego-motion estimation is an important step towards fully autonomous mobile robots. In this paper we propose the use of an initial but automatic camera tilt calibration, which transforms the subsequent motion estimation to a 2D rigid body motion problem. This transformed problem is solved ℓ_2-optimally using RANSAC and a two-point method for rigid body motion. The method is experimentally evaluated using a camera mounted onto a mobile platform. The results are compared to measurements from a highly accurate external camera positioning system which are used as gold standard. The experiments show promising results on real data.

1 INTRODUCTION

One of the fundamental problems in robotics research is how to use various sensor data to estimate accurately the position and motion of a mobile robot. The solution to this problem will by necessity depend heavily on various application specific considerations, such as the type and quality of the sensors employed and the environment in which the robot is intended to operate. Many of the successful approaches to this problem have been formulated in the framework of *Simultaneous Localisation and Mapping* (SLAM), where the robot estimates a map of its surroundings as well as its own position with respect to this map. What is considered a suitable representation of the map is also application specific, and can range from sparse clouds of feature points to dense and textured 3D models.

The early methods for SLAM were focused on sensors such as wheel encoders and laser range finders, and how to use statistical estimation and filtering techniques to determine ego-motion and relative position from such data. The probabilistic viewpoint has proven to be a suitable framework for visual SLAM as well, and has remained popular from pioneering works such as those by Harris and Pike (1988) and by Durrant-Whyte (1987) to more recent methods such as the vSLAM system by Karlsson et al. (2005) and the MonoSLAM system by Davison et al. (2007). In this type of algorithms, Kalman filters and particle filters (Gustafsson, 2012) are popular choices, and are often used e.g. to include a kinematic motion model or to combine data from different sensors.

An important sub-problem in SLAM deals with *Loop Closure*, where the goal is to join spatially close but temporally distant areas of the map. Being able to detect loops typically allows a drastic reduction in the accumulated positioning error, as demonstrated by e.g. Newman and Ho (2005) and Jones and Soatto (2011). However, if the loops are allowed to be of arbitrary length, the storage of, and comparison against, an increasingly large map becomes inhibiting both in terms of storage and computation time.

On the other end of the spectrum are the so called odometry methods, in which the map comprises only very recent information that is used for local estimation of relative position. The study of these methods is important because they must be used if no loop has yet been detected, or if for some reason loop closure is not a viable option. When cameras are the primary sensors used in an odometry method, as in this present paper, it is often referred to as *Visual Odometry* (VO).

In many practical cases, especially for ground robots in indoor environments, the motion of the robot is constrained to a plane parallel to the floor. By considering methods which explicitly assume planar motion, the vertical positioning error of the attached sensors will automatically be bounded over arbitrarily long motion sequences. This insight has successfully been utilised in several visual navigation systems such as Ortín and Montiel (2001), Hajjdiab and Laganière (2004), Liang and Pears (2002), Scaramuzza (2011a,b), and Zienkiewicz and Davison (2015).

WadenbÃďck M., Karlsson M., Heyden A., Robertsson A. and Johansson R.
Visual Odometry from Two Point Correspondences and Initial Automatic Camera Tilt Calibration.
DOI: 10.5220/0006079903400346
In *Proceedings of the 12th International Joint Conference on Computer Vision, Imaging and Computer Graphics Theory and Applications (VISIGRAPP 2017)*, pages 340-346
ISBN: 978-989-758-227-1

Figure 1: Sample images from the positioning experiments. We assume that there is some perceivable structure in the floor, but otherwise no particular preparation of the environment is necessary. This is mainly a requirement for the feature detector, rather than for the proposed method itself.

Ortín and Montiel consider the epipolar geometry derived from planar camera motion, and propose both a linear three-point method and a non-linear two-point method to estimate this type of camera motion (Ortín and Montiel, 2001). The method requires the camera to be mounted with the y-axis vertical with high accuracy, which is achieved by means of a spirit level. Neither of the methods presented in their paper determine the relative length of the translation, which therefore must be determined in some other way.

Essentially the same motion parametrisation was used in the approach proposed by Scaramuzza, but with an additional nonholonomic constraint based on the assumption that the local motion is a circular motion (Scaramuzza, 2011a,b). Because of this additional constraint, the local motion can be estimated from only one point correspondence, which allows for a very efficient outlier removal based on histogram voting. The approach is evaluated on relatively long motion sequences captured from a camera mounted onto a car. Despite its many advantages, the method shares the same weakness as Ortín and Montiel (2001) that the camera orientation must be known, and no efficient way to calibrate this is presented. Furthermore, though the nonholonomic constraint may be valid in automotive applications, it is not valid for robots with omnidirectional wheels (e.g. robots such as the Fraunhofer IPA rob@work platform shown in Figure 3).

In contrast to the two previously mentioned methods, Zienkiewicz and Davison use a dense matching of the whole image in order to determine the full camera pose (Zienkiewicz and Davison, 2015). The method is demonstrated to perform well under a large number of different conditions. Since the camera pose is computed during the registration of the images, no effort must be spent in order to mount the camera in a particular way. The method relies on an efficient implementation on a GPU in order to cope with the heavy computations involved in performing the dense registration.

The problem addressed in the present paper is the determination of orientation and position of a mobile robot during a motion sequence. Our goal is to use images from a camera mounted onto a mobile robot in an unknown but rigid downward direction, together with the assumption of planar motion to provide accurate estimates of the local robot motion. Our method does not yet perform any filtering techniques or nonlinear optimisation over several frames, but focuses entirely on estimating the local motion. Some sample images captured by the camera under these conditions are shown in Figure 1.

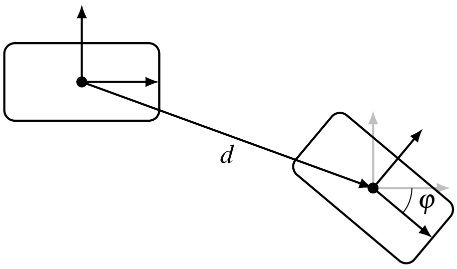

Figure 2: Illustration of the two-dimensional rigid body motion under consideration. The motion of the platform is described by a displacement d and a rotation an angle φ around the plane normal.

The idea presented in this paper is to transform the motion of the feature points into a 2D rigid body motion problem, which is solved ℓ_2-optimally using a decoupling of the determination of rotation and translation proposed by Arun, Huang and Blostein (1987). This transformation of the problem is achieved by performing an initial determination of the camera tilt using the method by Wadenbäck and Heyden (2014). This initial and automatic tilt calibration allows the camera to be mounted onto the robot in an arbitrary downward direction, and allows the subsequent motion estimates to be computed directly from the feature points instead of from a homography or essential matrix.

2 METHOD

Our method relies on corresponding feature points in the images, which need to be reliably detected and matched. The selection of algorithms for this particular sub-problem is beyond the scope of this paper. In our experiments we used SURF features (Bay, Tuytelaars and Van Gool, 2006), which were matched using the approximate nearest neighbour matching (Muja and Lowe, 2009, 2014). This selection is not based on a thorough evaluation of the alternatives, but it does provide sufficiently useful point correspondences for the method we present.

2.1 Camera Parametrisation

Assuming the standard model of the pinhole perspective camera (see Hartley and Zisserman (2004) for an in-depth discussion), with known and constant intrinsic parameters, the normalised camera projection matrix associated with an image taken at position $d = (d_1, d_2, d_3)$ will be

$$P = R(\psi, \theta, \varphi)[I \mid -d]. \tag{1}$$

Here, (ψ, θ, φ) are Tait-Bryan angles[1] defining the orientation through the rotation matrix

$$R(\psi, \theta, \varphi) = R_x(\psi)R_y(\theta)R_z(\varphi), \tag{2}$$

where each of R_x, R_y, and R_z denotes a rotation about its corresponding coordinate axis. In this work ψ and θ are unknown but constant, whereas φ and d may vary from image to image. We furthermore assume that the camera moves in the plane $z = 0$ (i.e. we always have $d_3 = 0$), and that the floor plane is $z = 1$. These assumptions do not constrain the model, because they only reflect our choice of global coordinate frame.

2.2 Tilt Estimation

In this section we present a brief review of the tilt estimation scheme in Wadenbäck and Heyden (2014). Without loss of generality, the camera projection matrices associated with two images may be written as

$$\begin{cases} P = R_{\psi\theta}[I \mid 0] \\ P' = R_{\psi\theta}R_z(\varphi)[I \mid -d], \end{cases} \tag{3}$$

where $R_{\psi\theta} = R(\psi, \theta, 0)$ is the unknown camera tilt. From (3) it follows that the inter-image homography will be of the form

$$H = R_{\psi\theta}R_z(\varphi)(I - dn^T)R_{\psi\theta}^T, \tag{4}$$

where $n = (0, 0, 1)$ is a normal to the floor. As a consequence,

$$R_{\psi\theta}^T H^T H R_{\psi\theta} = (I - dn^T)^T (I - dn^T). \tag{5}$$

In this matrix equation, it turns out that some elements depend only on ψ and θ. Denoting the left hand side of (5) by L, one obtains two non-linear equations

$$\begin{cases} L_{11} - L_{22} = 0 \\ \qquad L_{12} = 0. \end{cases} \tag{6}$$

Wadenbäck and Heyden proposed a coordinate descent-like method where in each iteration (6) became a linear system of equations in the trigonometric functions. This allows several homographies of the type (4) to be used simultaneously in the estimation by simply stacking the linear systems, which improves robustness and accuracy.

For this tilt estimation method to succeed, it is assumed that for most of the homographies used the translation vector d and the angle φ are not both zero, otherwise the tilt angles ψ and θ are not well defined. If indeed d and φ are both zero, the homography matrix will be a scalar multiple of the identity matrix, and this case is thus easily and efficiently detected by a separate check. This situation arises in practice, since the robot may at times stop during the motion, e.g. to await new commands or to avoid collision with obstacles.

2.3 Motion Estimation

Suppose $x'_j \leftrightarrow x_j$, $j = 1, \ldots, N$ are point correspondences between the first and second image, expressed in homogeneous coordinates. These must satisfy

$$\begin{aligned} x'_j &\sim Hx_j \Leftrightarrow \\ R_{\psi\theta}^T x'_j &\sim R_z(\varphi)(I - dn^T)R_{\psi\theta}^T x_j. \end{aligned} \tag{7}$$

After the tilt has been determined as explained in Section 2.2, we consider $R_{\psi\theta}$ to be known. Introducing

$$y_j \sim R_{\psi\theta}^T x_j \qquad \text{and} \qquad y'_j \sim R_{\psi\theta}^T x'_j, \tag{8}$$

and using the representation with last coordinate equal to one, (7) becomes a planar rigid body motion in terms of $z_j = \pi y_j$ and $z'_j = \pi y'_j$. Here π denotes an orthogonal projection onto the first two coordinates, i.e.

$$\pi = \begin{bmatrix} 1 & 0 & 0 \\ 0 & 1 & 0 \end{bmatrix}. \tag{9}$$

If all point correspondences are correct, i.e. no outliers are present, this may be solved directly in a least squares sense using an adaptation to 2D of the method presented in Arun, Huang and Blostein (1987). The 2D version of this problem is well-posed if at least two point correspondences are used, and the solution gives an estimate of φ and d.

The least squares solution to the rigid body motion problem presented in Arun, Huang and Blostein

[1] In the whole of this paper we will consider angles as equivalence classes, where angles differing with additive multiples of 2π belong to the same class.

(1987) works by decoupling the translation and the rotation involved. It is shown that by forming

$$q_j = z_j - \frac{1}{N}\sum_{k=1}^{N} z_k \quad \text{and} \quad q'_j = z'_j - \frac{1}{N}\sum_{k=1}^{N} z'_k, \tag{10}$$

the optimal rotation matrix is VU^T, where $M = U\Sigma V^T$ is a singular value decomposition of

$$M = \sum_{j=1}^{N} q_j (q'_j)^T. \tag{11}$$

The optimal estimate $d^*_{2\mathrm{D}}$ of the 2D translation vector will then be

$$d^*_{2\mathrm{D}} = \left(\frac{1}{N}\sum_{k=1}^{N} z'_k\right) - VU^T\left(\frac{1}{N}\sum_{k=1}^{N} z_k\right), \tag{12}$$

and to get the 3D translation a zero should be appended as the third coordinate.

Since the point correspondences are found by automatically matching the feature points, there will typically be many incorrect matches, and a robust estimation framework should be used. For this reason, we employ the RANSAC framework (Fischler and Bolles, 1981) to fit the rigid body motion to random samples containing two point correspondences. In each RANSAC iteration, a motion model is determined from two point correspondences, and for all other point correspondences the difference between the forward mapped points and the points observed in the second image are computed. Here, points with a transfer error greater than a certain threshold, typically expressed in terms of the standard deviation, are regarded as outliers. In our experiments, a threshold of one standard deviation worked well for the outlier removal. After a suitable inlier set has been determined, the final motion model is determined using the rigid body motion estimation method described above with all the inliers.

3 EXPERIMENTS

During the experiments, a mobile robot of model Fraunhofer IPA rob@work (base platform) (Fraunhofer IPA, 2012) was used. The platform, shown in Figure 3, has omnidirectional wheels, allowing it to perform pure translations and pure rotations, as well as combinations of these. A camera was attached to the undercarriage, directed down towards the floor plane and recording at approximately ten frames per second.

The tilt angles were determined from the first few non-identity homographies, on which the tilt estimation described in Section 2.2 was applied, and were used for the remainder of the motion sequence. Since the camera was mounted slightly differently in the different experiments, the tilt calibration had to be performed for each experiment. In our experience, the tilt estimation reached convergence after about 15-20 frames (roughly 2 s of motion), as can be seen in Figure 4.

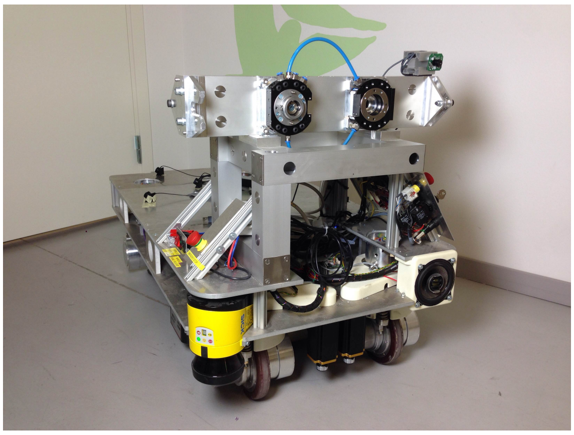

Figure 3: The experiments were carried out on a mobile robot of model Fraunhofer IPA rob@work (base platform).

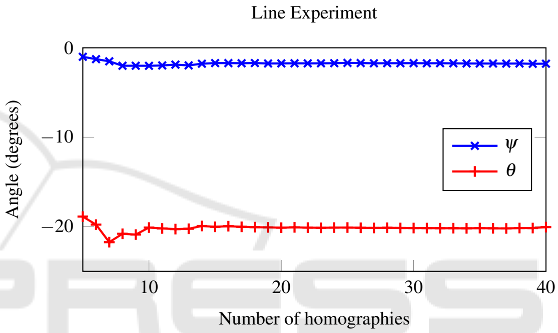

Figure 4: The tilt estimation reached convergence after about 15-20 frames (roughly 2 s of motion). Since the tilt estimation problem is ill-posed for very small translations, using fewer than five images did not give reasonable estimates with the current frame rate and velocity.

3.1 Evaluation Against Gold Standard

For the experiments presented in this section, a highly accurate optical tracking system of model K600 from Nikon Metrology (Nikon Corporation, 2011) was used for reference and served as gold standard for the platform position. This system provides an absolute accuracy of less than 100 µm, and was sampled at the rate 250 Hz. In addition to the camera shown in Figure 5(a), the tracking system consists of a number of LEDs mounted on the robot, for the Nikon Metrology camera to track.

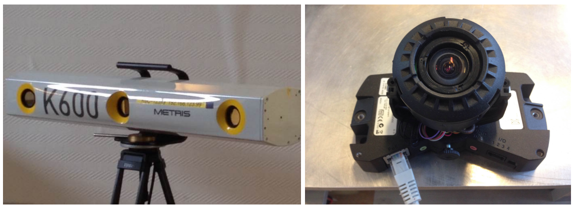

(a) Nikon Metrology K600 (b) Axis P3364-VE

Figure 5: The stationary Nikon Metrology K600 camera (a) used to measure the gold standard positions in the experiments. This is not to be confused with the (Axis Communications AB, 2012) (b) that was mounted on the mobile robot and used for the VO.

During these positioning experiments, the mobile robot moved in three different motion patterns described below.

1. Translation along a straight line with constant orientation.
2. Translation forward, followed by translation to the right, in the robot's own frame. Again, the orientation was kept constant. This motion is possible due to the omnidirectional wheels of the robot, and resembles an effective version of parallel parking.
3. Translation combined with rotation (light turn). The robot moved forward in relation to its own frame, while rotating to the right, which resulted in a curved path.

The motion patterns may be viewed in Figure 6, and the positioning errors in relation to travelled distance are shown in Figure 7. The average absolute position error was 2.3 mm, 5.0 mm and 8.7 mm, for the trials consisting of a straight line, parallel parking, and turn, respectively.

3.2 Evaluation on a Longer Sequence

We also tried a slightly longer motion sequence, shaped approximately as an ellipse, with a total length of about 5.75 m and in which the robot made a full turn. The robot was driven in such a way so as to introduce some small irregularities to the trajectory, and such that the images at the starting position and the final position were overlapping. Due to range and workspace limitations in the Nikon system, there is no gold standard data for this experiment. Instead, the images from the starting position and the final position were used to determine the true final position, which was then compared to the final positions estimated by the VO approach.

The result from this experiment is shown in Figure 8 and Figure 9. The position error in the final position, as determined by comparing the first and final image as explained above, was found to be 0.71 % of the travelled distance.

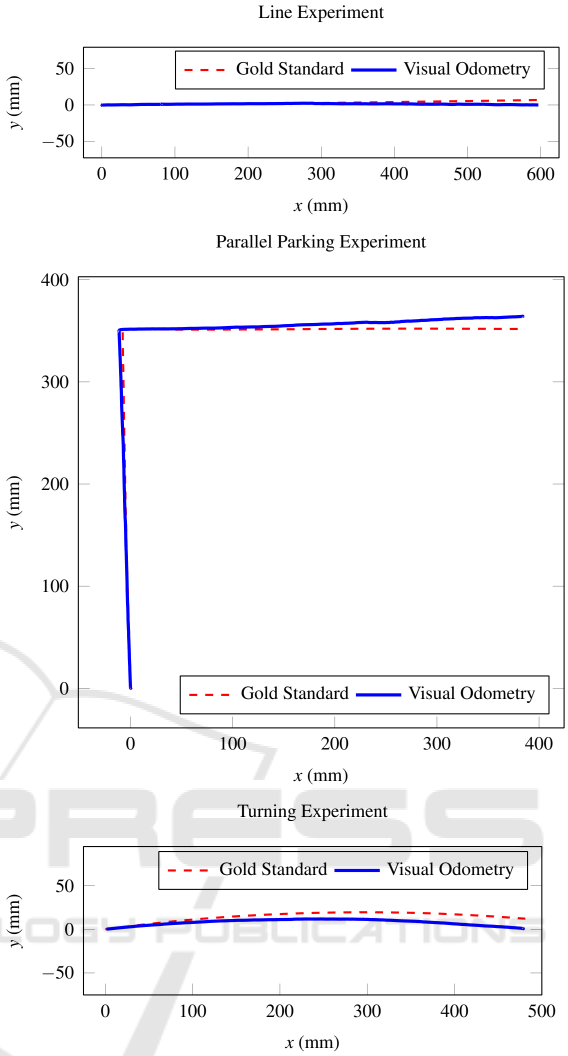

Figure 6: True and estimated positions, using VO. The figure shows the motions in the same order as they are described in the text, i.e. straight line (top), parallel parking (middle), and light turn (bottom). See also Figure 7, where the position errors in relation to travelled distance are shown.

4 DISCUSSION

The positioning provides good estimates locally, but like all dead reckoning approaches, the accuracy deteriorates with the travelled distance. Sources of error include inaccuracies in the intrinsic camera calibration, noise and outliers influence in the feature point matching, as well as limited image resolution. Addi-

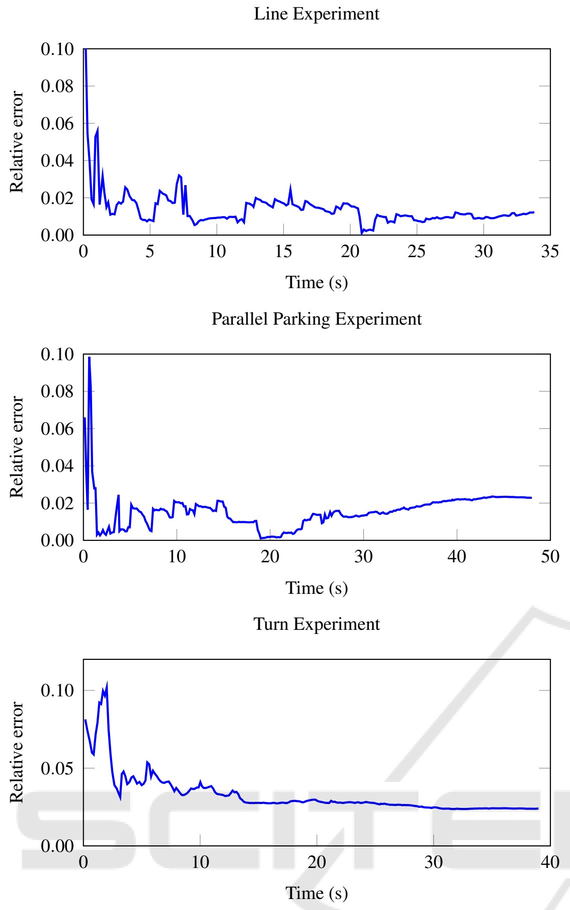

Figure 7: Relative estimation error, formed by dividing the absolute error with travelled distance. The figure shows the motions in the same order as they are described in the text and in Figure 6.

tional sources are the carriage suspension and imperfections in the ground surface, which may invalidate the planar motion assumption.

It remains as future work to extend this method by considering map building parallel to the positioning in order to improve the performance over longer distances, and to employ filtering techniques or nonlinear optimisation over several frames. Furthermore, one could include sensors such as laser range finders, to avoid the problem with pure dead reckoning.

5 CONCLUSIONS

In this paper we have proposed and evaluated a VO approach based on 2D rigid body motion. The method relies on an initial estimation of the camera tilt, which we have demonstrated can be achieved from a short automatic calibration process. After the tilt calibration, a rigid body motion problem is solved robustly using RANSAC and a two-point method, which finally gives an ℓ_2-optimal fit to the inliers. The method has been evaluated experimentally, and was demonstrated to achieve high positioning accuracy. This paper additionally provided experimental verification of the work in Wadenbäck and Heyden (2014) on real image data.

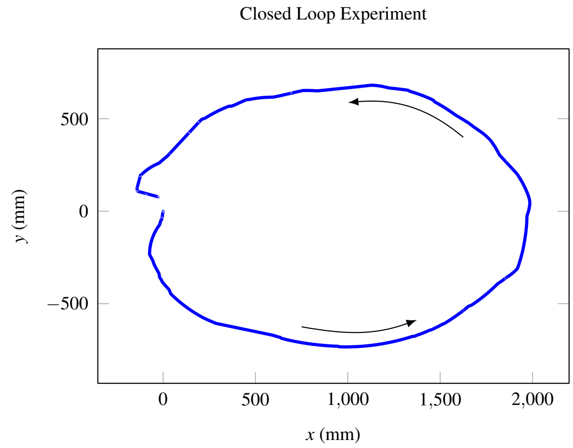

Figure 8: Trajectory estimated using VO. Here the trajectory has been scaled and is shown in the true scale, although this scale cannot be determined from the images alone.

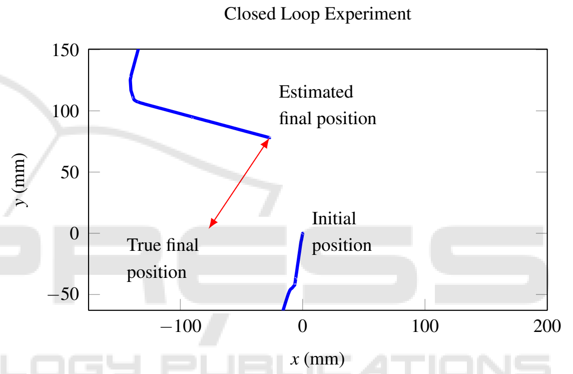

Figure 9: Close-up of the trajectory in Figure 8, showing the initial and final position.

ACKNOWLEDGMENTS

This work has been partly funded by the Swedish Foundation for Strategic Research through the SSF project ENGROSS (www.engross.lth.se). Among the authors are members of the LCCC Linnaeus Center and the ELLIIT Excellence Center at Lund University.

REFERENCES

Arun, K. S., T. S. Huang and S. D. Blostein (1987). “Least Squares Fitting of Two 3-D Point Sets”. In: *IEEE Transactions on Pattern Analysis and Machine Intelligence* 9(5), pp. 698–700.

Axis Communications AB (2012). *AXIS P3364-VE Network Camera*. URL: http://www.axis.com/global/en/products/axis-p3364-ve (visited on 27/02/2016).

Bay, H., T. Tuytelaars and L. Van Gool (2006). “SURF: Speeded Up Robust Features”. In: *Proceedings of the 9th European Conference on Computer Vision (ECCV)*. Vol. 3951. in series *Lecture Notes in Computer Science*. Graz, Austria: Springer-Verlag, pp. 404–417.

Davison, A. J., I. D. Reid, N. D. Molton and O. Stasse (2007). “MonoSLAM: Real-Time Single Camera SLAM”. In: *IEEE Transactions on Pattern Analysis and Machine Intelligence* 29(6), pp. 1052–1067.

Durrant-Whyte, H. F. (1987). “Consistent Integration and Propagation of Disparate Sensor Observations”. In: *The International Journal of Robotics Research* 6(3), pp. 3–24.

Fischler, M. A. and R. C. Bolles (1981). “Random Sample Consensus: A Paradigm for Model Fitting with Applications to Image Analysis and Automated Cartography”. In: *Communications of the ACM* 24(6), pp. 381–395.

Fraunhofer IPA (2012). *Compact Drive Modules for Omnidirectional Robot Platforms*. URL: http://www.care-o-bot.de/en/rob-work.html (visited on 26/02/2016).

Gustafsson, F. (2012). *Statistical Sensor Fusion*. Second ed. Lund, Sweden: Studentlitteratur AB.

Hajjdiab, H. and R. Laganière (2004). “Vision-based Multi-Robot Simultaneous Localization and Mapping”. In: *Proceedings of the 1st Canadian Conference on Computer and Robot Vision (CRV)*. London, ON, Canada: IEEE Computer Society, pp. 155–162.

Proceedings of the IEEE International Conference on Robotics and Automation (ICRA) (2005). Barcelona, Spain: IEEE Robotics and Automation Society.

Harris, C. G. and J. M. Pike (1988). “3D Positional Integration from Image Sequences”. In: *Image and Vision Computing* 6(2), pp. 87–90.

Hartley, R. I. and A. Zisserman (2004). *Multiple View Geometry in Computer Vision*. Second ed. Cambridge, England, UK: Cambridge University Press.

Jones, E. S. and S. Soatto (2011). “Visual-inertial navigation, mapping and localization: A scalable real-time causal approach”. In: *The International Journal of Robotics Research* 30(4), pp. 407–430.

Karlsson, N. et al. (2005). “The vSLAM Algorithm for Robust Localization and Mapping”. In: *Proceedings of the IEEE International Conference on Robotics and Automation (ICRA)*. Barcelona, Spain: IEEE Robotics and Automation Society, pp. 24–29.

Liang, B. and N. Pears (2002). “Visual Navigation using Planar Homographies”. In: *Proceedings of the IEEE International Conference on Robotics and Automation (ICRA)*. Vol. 1.Washington, DC, USA: IEEE Robotics and Automation Society, pp. 205–210.

Muja, M. and D. G. Lowe (2009). “Fast Approximate Nearest Neighbors with Automatic Algorithm Configuration”. In: *Proceedings of the Fourth International Conference on Computer Vision Theory and Applications (VISAPP)*. Vol. 1. Lisbon, Portugal: INSTICC Press, pp. 331–340.

Muja, M. and D. G. Lowe (2014). “Scalable Nearest Neighbor Algorithms for High Dimensional Data”. In: *IEEE Transactions on Pattern Analysis and Machine Intelligence* 36(11), pp. 2227–2240.

Newman, P. and K. Ho (2005). “SLAM- Loop Closing with Visually Salient Features”. In: *Proceedings of the IEEE International Conference on Robotics and Automation (ICRA)*. Barcelona, Spain: IEEE Robotics and Automation Society, pp. 635–642.

Nikon Corporation (2011). *K-Series Optical CMM solutions – supporting a variety of metrology applocations*. URL: http://www.nikonmetrology.com (visited on 26/02/2016).

Ortín, D. and J. M. M. Montiel (2001). “Indoor robot motion based on monocular images”. In: *Robotica* 19(3), pp. 331–342.

Scaramuzza, D. (2011a). “1-Point-RANSAC Structure from Motion for Vehicle-Mounted Cameras by Exploiting Non-holonomic Constraints”. In: *International Journal of Computer Vision* 95(1), pp. 74–85.

Scaramuzza, D. (2011b). “Performance Evaluation of 1-Point-RANSAC Visual Odometry”. In: *Journal of Field Robotics* 28(5), pp. 792–811.

Wadenbäck, M. and A. Heyden (2014). “Ego-Motion Recovery and Robust Tilt Estimation for Planar Motion Using Several Homographies”. In: *Proceedings of the 9th International Conference on Computer Vision Theory and Applications (VISAPP)*. Vol. 3. Lisbon, Portugal: SCITEPRESS, pp. 635–639.

Zienkiewicz, J. and A. J. Davison (2015). “Extrinsics Autocalibration for Dense Planar Visual Odometry”. In: *Journal of Field Robotics* 32(5), pp. 803–825.